

# Experimental Test Setup of an Airwall to Reduce the Convective Heat Loss in Solar Thermal Cavity Receivers

Moritz Bitterling<sup>1</sup>[\[https://orcid.org/0009-0001-9158-7980\]](https://orcid.org/0009-0001-9158-7980), Gregor Bern<sup>1</sup>[\[https://orcid.org/0000-0002-5024-7699\]](https://orcid.org/0000-0002-5024-7699),  
Hannes Fugmann<sup>1</sup>[\[https://orcid.org/0000-0002-5177-9072\]](https://orcid.org/0000-0002-5177-9072), Martin Karl, Christopher Cohnen<sup>2</sup>,  
Thomas Sonnabend<sup>2</sup>, and Thomas Fluri<sup>1</sup>[\[https://orcid.org/0000-0001-8022-0369\]](https://orcid.org/0000-0001-8022-0369)

<sup>1</sup> Fraunhofer Institute for Solar Energy Systems ISE, Germany

<sup>2</sup> LWT GmbH, Mönchengladbach, Germany

**Abstract.** An experimental setup is presented which allows to experimentally determine the thermal heat losses from a heated solar cavity receiver with an airwall. The setup is a ‘near-full-scale’ replica of a receiver, which ensures that the characteristic fluid dynamic numbers are in a range relevant for practical industrial applications. The executed tests show that – at ideal configuration – the airwall can reduce the overall thermal losses by  $7\pm 2\%$ . The reduction of the convective losses amounts to  $32\pm 11\%$ , which is in line with the known predictions from CFD simulations.

**Keywords:** Central Receiver, Heat Loss, Air Curtain, Airwall, Convection

## 1. Introduction

In Central Cavity Receiver CSP Systems, the thermal losses at the receiver are responsible for a large reduction of the optical-to-thermal efficiency. Heat loss due to heat radiation from the receiver surface accounts for most of the losses (approx. 60-80%), but it is challenging to avoid. However, convective losses also account for a considerable share of 20-40% of the losses, depending on the operation temperature. Different solutions have been proposed to prevent these losses: install a transparent window (e.g., made from quartz) [1], which potentially would entirely eliminate convection losses. Due to the challenge of producing a quartz window of the required size and durability, an array of quartz tube segments compiling the window has been proposed [2]. Alternatively, an airwall was proposed as a transparent shield for the cavity. In this concept, the inside of the cavity is separated from the colder environment by a slim but powerful air jet. The airwall concept has been simulated numerically [3, 4, 5] and it was also tested experimentally [6, 7], but to our knowledge no industrial-scale tests have been carried out yet. To be able to draw reliable conclusions from an experiment, the relevant characteristic numbers (Grashof, Reynolds, Richardson) of the test setup need to be similar to those of the real scale system.

In this work, a ‘near-full-scale’ replica of a cavity receiver equipped with an airwall system is presented. This setup allows simulating real operating conditions with a panel of electric heating elements. Tests are carried out to experimentally quantify the possible reduction of the convective heat losses and to assess the expected increase in receiver thermal performance. As a result, the overall energetic benefit of installing an airwall in a small central cavity receiver system can be reliably determined.

## 2. Methodology

### 2.1 Experimental setup

Prior to the design of the experimental setup, CFD simulations of a cavity with heated rear wall and shielded with an airwall were conducted (Fig. 1). However, due to observed numerical instabilities of the model, it was considered that the conclusions drawn from the simulations cannot be directly transferred to the real situation. For a reliable assessment of the benefit of an airwall for the thermal insulation of a cavity receiver, it was decided that a replica of a cavity receiver shall be built (Fig. 2, left) and equipped with an airwall (Fig. 2, right).

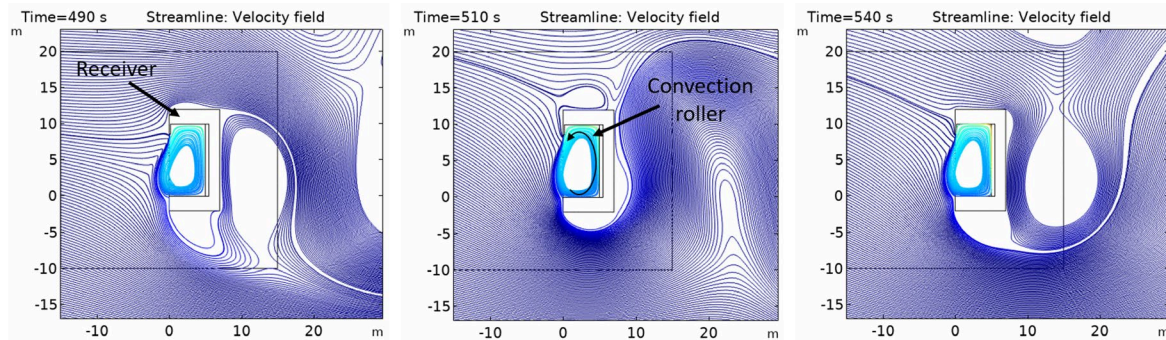


**Figure 1.** Numerical 2D simulation of air temperature and streamlines in and around the cavity receiver when the airwall is in operation. The CFD simulations were conducted to support the design of the test setup.



**Figure 2.** Construction and mounting of an experimental replica of a solar thermal cavity receiver (aperture area  $3 \times 3 \text{ m}^2$ ) in Freiburg. The nozzles of the airwall are mounted above and below the receiver opening (right image). With a panel of electrical heaters on the rear wall, realistic operating conditions of a receiver can be simulated. The present set-up is used to investigate the possible extent of reduction of the convective losses through the airwall and thus determine its effect on the overall receiver efficiency.

For the design of the cavity regarding technical and electrical aspects, the work of Kraabel [8] served as a guideline. In Fig. 3, a sketch of the setup is shown. The designed cavity has an aperture opening of 286x300 cm<sup>2</sup> and a depth of 200 cm. A panel of 21 plane electrical heating elements, with a maximum heating power of 12 kW each, is used to simulate the hot absorber surface at the inner rear side of the cube. With the present power supply and the available 2-step temperature control unit, a surface temperature of 650 °C can be reached. The five walls of the steel cube are insulated with ceramic fiber and rock wool with 15 cm thickness (rear wall) and 10 cm otherwise. K-type thermocouples are placed on the surface of each heating element and their signal is used as the set point for the temperature control of seven independent heating zones. In addition, 24 thermocouples are arranged in the cavity to monitor the temperature of the atmosphere inside. The AC heating current of each of the seven thermal zones (with three heating elements each) is monitored with current probes, which allows continuous measurement of the electrical heating power. A cup anemometer at the top of the scaffolding measures the wind speed.

The whole setup can be tilted forwards, to be able to simulate inclined cavities that create the stagnant zone at the top of the cavity. Furthermore, the rear wall may be moved forward to test the effect of the airwall on an external receiver.

The design of the blower and the airwall allows to reach a variable air outlet velocity of up to 30 m/s. The rotation of the air nozzles can be adjusted to identify the flow conditions which result in the best convective insulation. A fog machine can visualize the airflow.

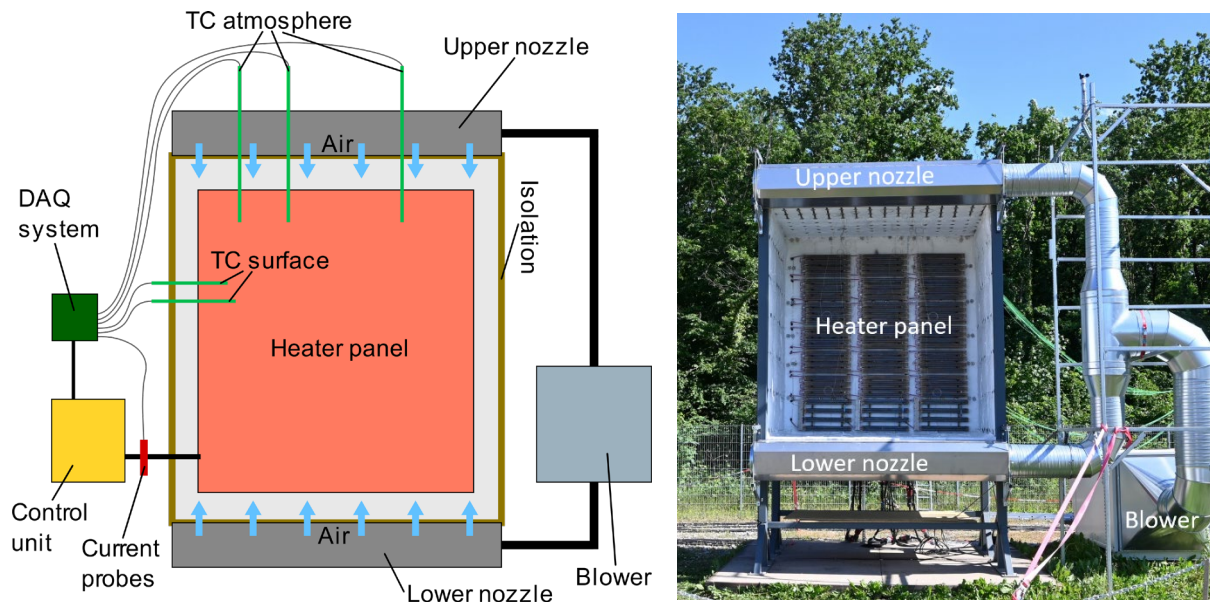


**Figure 3.** Left: Sketch of the experimental setup used for the airwall tests. The thermal control unit can be used to set a surface temperature of up to 650 °C for the panel of electric heaters on the rear wall of the insulated cube. A data acquisition system records the heating current from current probes. Surface and atmospheric temperatures are monitored with 45 thermocouples. The installed blower generates a flow of air which is released through two nozzles at the top and bottom front edge of the cube, creating an airwall that serves as transparent shield for the opening of the cavity. Right: Image of the completed measurement setup in Freiburg, Germany.

## 2.2. Execution of the tests

During the tests, the temperature of each central thermocouple of the seven thermal zones was kept at 610 °C by a 2-step controller for the electrical current. The electrical power required to maintain this temperature was determined by continuously measuring the electrical current. In stationary conditions, this power is equivalent to the combined conductive (through the walls), radiative, and convective thermal losses of the cavity. Due to the statistical fluctuations of the 2-step controller, measurements must be made over a relatively long period of time to obtain significant results.

To measure the baseline scenario – the overall heat loss without airwall –, the setup was operated for 45 minutes at design temperature (Fig. 4). After that, the blower for the airwall was switched on and its power increased in 5 steps to up to 2 kW. The measurements at each step were taken for 30 minutes. The measurement campaign was carried out at night to minimize the influence of fluctuating wind on the measurement results. The maximum ambient wind speed during the tests was less than 0.5 m/s.



**Figure 4.** Test of the thermal losses of the cavity with and without airwall. The temperature of the rear wall is kept constant at 610 °C. In stationary conditions, the required electrical heating power is equivalent to the thermal losses of the cube. If the system is operated with ideal airwall parameters, the required heating power can be significantly reduced.

To have a better understanding of the air flow conditions that occur at the cavity, a fog machine was used to visualize the air outflow from the upper and lower nozzle (Fig. 5). A well-defined zone of a fast air jet forms in front of the cavity, with little exchange with the air volume inside. Due to the convective updraft inside the cavity, the upper part of the airwall is pressed slightly outward, and the lower part is sucked in.



**Figure 5.** Visualization of the well-defined airwall in front of the cavity with a fog machine. During this test, the air blower was running with medium power (0.9 kW). Fog is introduced through the blower into the upper and lower air nozzle, which are mounted above and below the opening of the cavity. The images were taken about every second to capture the progressive fog propagation.

### 3. Results

Fig. 6 shows the heating power required to maintain a constant surface temperature during the test (top) and the corresponding power of the air blower (bottom). As the individual power measurements fluctuate strongly due to the statistical nature of the 2-step controller, 2- and 15-minutes moving averages are shown as well as the mean value (orange) of each segment of the test.

In the base case without airwall (minutes 0-45), the power is  $P_{\text{base}} = 181 \pm 2$  kW. After switching on the airwall, the power drops significantly, and its minimum is reached during the third step (minutes 75-105) with a heating power of  $168 \pm 3$  kW. Since the heater temperatures in the cavity do not change significantly during the test (mean standard deviation of the temperatures of the seven controlled thermocouples: 1.7 K), the radiative and conductive losses remain constant. This means that the reduction in heating power is caused only by the positive effect of the airwall operation on the convective losses. The achieved power reduction amounts to  $13 \pm 4$  kW or  $7.1 \pm 1.9\%$  of the total thermal losses.

A further increase of the air blower power causes the convective losses to rise again. If the power is very high (minutes 165-195), the convective losses are even higher than in the base case.

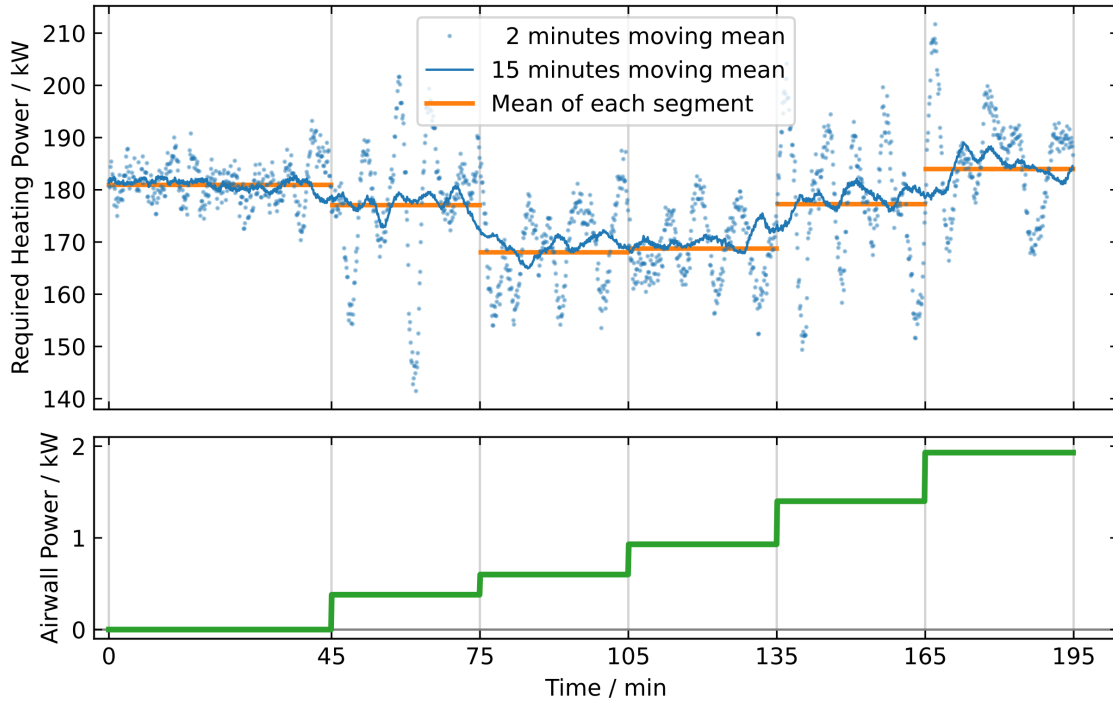


**Figure 6.** Required heating power to maintain a constant temperature in the cavity (top). 2- and 15-minutes moving averages are shown as well as the mean of each entire segment of the measurements (orange). The base case (without airwall) is from minute 0-45. During the tests, the power of the airwall blower (bottom) was gradually increased to identify the ideal level. The observed decrease in the heating power is caused by a reduction of the convective losses due to the operation of the airwall. The optimum is reached in step 3 (minutes 75-105). If the power of the airwall is set too high, the convective losses increase to a level even higher than in the case without airwall.

An experimental separation of the different thermal loss mechanisms (radiative, conductive, convective) was not performed and remains to future experimental evaluation. But with the help of the theoretical models, this separation can be made (with some uncertainty) on the basis of the known geometrical and material parameters of the setup. The information about the magnitude of the radiative and conductive losses can then be used to determine the relative reduction of the convective losses.

The Stefan–Boltzmann law yields for the radiative loss (with the high uncertainty caused by the uncertainty of the emissivity of the heating elements, and of the surface temperature distribution over the entire heater panel)

$$P_{\text{rad}} = 138 \pm 8 \text{ kW} \quad (1)$$

and the conductive losses through the insulated walls amount to

$$P_{\text{cond}} = 3 \pm 1 \text{ kW} . \quad (2)$$

With

$$P_{\text{base}} = P_{\text{rad}} + P_{\text{cond}} + P_{\text{conv}} , \quad (3)$$

this yields for the convective losses (in the base case without airwall)

$$P_{\text{conv}} = 40 \pm 8 \text{ kW} . \quad (4)$$

This value implies that the reduction of the convective losses by  $13 \pm 4$  kW is a relative reduction by  $32 \pm 11\%$ . Fig. 7 visualizes the relationships and the inherent uncertainty in the theoretical model of the radiative and conductive losses.

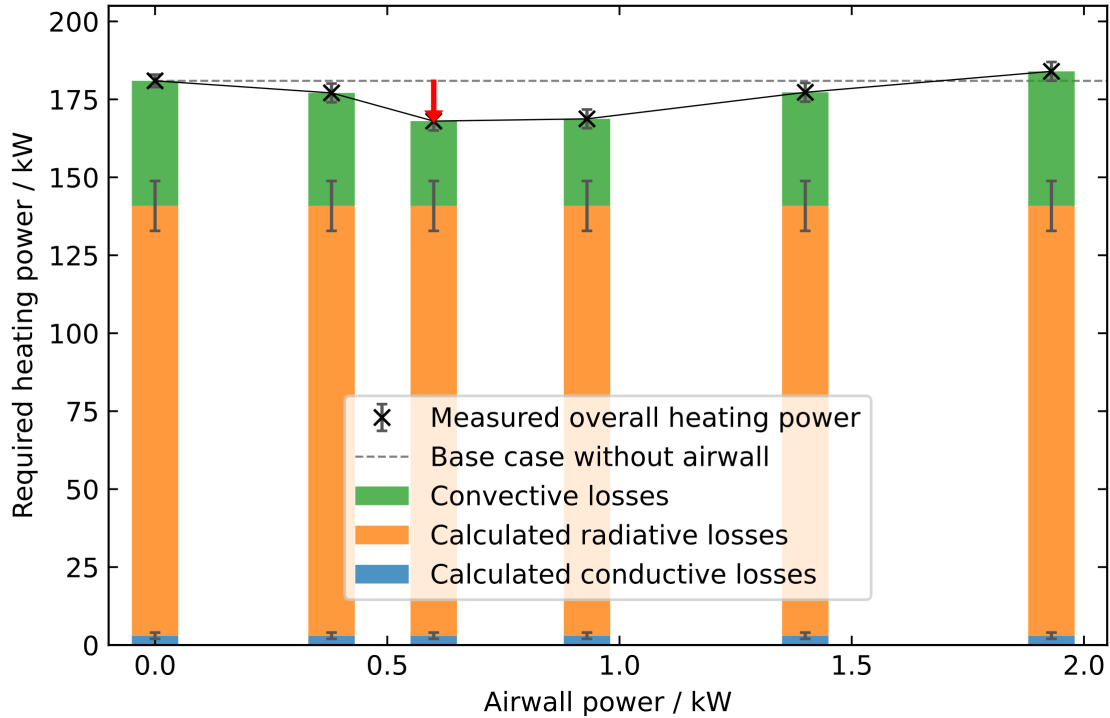


**Figure 7.** Separation of the thermal losses of the cavity as a function of airwall power. The crosses show the measured heating power (equal to the thermal losses) for different air blower power. Theoretical models were used to separate the total heat loss into the conductive, radiative, and convective components. In the optimal case (airwall power 0.6 kW), the reduction of the convective losses (red arrow) is  $7.1 \pm 1.9\%$  of the overall thermal losses or  $32 \pm 11\%$  of pure convective losses.

#### 4. Conclusions and Outlook

The observed experimental reduction of the convective losses of around 30% due to airwall operation is in line with the values based on numerical simulations [3, 4]. Since for the conducted experiments the setup was not yet fully optimized, there is reasonable expectation that slightly higher values will be achieved experimentally in the future. We expect a considerable optimization potential in the nozzle orientation and geometry and in the individual blow out speed of both nozzles. This will be the subject of future investigation. Moreover, the temperature control should be applied with a finer timing (pulse group control) and with improved control parameters to achieve more accurate results within shorter measurement time. Finally, the adjusted and upgraded setup will be used to precisely study the influence of wind on the performance of the airwall.

In summary, the reduction of thermal losses of the observed magnitude (32% of the convective losses, 7% of total losses) gives a strong indication of the commercial and economic applicability of airwall technology in solar tower power plants. With further development, i.e. adaptation to wind conditions, the airwalls can become an economical and technically feasible alternative to windows for unpressurized receivers.

## Data availability statement

Data and supplementary material will be provided upon request.

## Author contributions

**M. Bitterling:** Conceptualization, Data curation, Formal analysis, Investigation, Methodology, Validation, Visualization, Writing – original draft. **G. Bern:** Conceptualization, Funding acquisition, Methodology, Project administration, Writing – review & editing. **H. Fugmann:** Software, Validation, Writing – review & editing. **M. Karl:** Conceptualization, Project administration, Writing – review & editing. **C. Cohnen:** Methodology, Resources. **T. Sonnabend:** Methodology, Resources. **T. Fluri:** Funding acquisition, Supervision, Writing – review & editing

## Competing interests

The authors declare no competing interests.

## Funding

The project, under which the work presented in this paper has been conducted, was funded by the German Federal Ministry for Economic Affairs and Climate Protection (BMWK) under code 0324174. The authors of this publication are responsible for its contents.

## References

1. J. Hertel, R. Uhlig, M. Söhn, C. Schenk, G. Hensch, H. Bornhöft, "Fused silica windows for solar receiver applications" AIP Conference Proceedings, vol. 1734, p. 030020, 2016, <https://doi.org/10.1063/1.4949072>
2. R. Buck, "Optical performance of segmented aperture windows for solar tower receivers" AIP Conference Proceedings, vol. 1850, p. 030006, 2017, <https://doi.org/10.1063/1.4984349>
3. R. Mondal, J. F. Torres, G. Hughes, J. Pye, "Air curtains for reduction of natural convection heat loss from a heated plate: A numerical investigation" Int. J. Heat Mass Transf., vol. 189, p. 122709, 2022, <https://doi.org/10.1016/j.ijheatmasstransfer.2022.122709>
4. J. Fang, N. Tu, J. F. Torres, J. Weia, J. D. Pye, "Numerical investigation of the natural convective heat loss of a solar central cavity receiver with air curtain" Appl. Therm. Eng., vol. 152, p. 147-159, 2019, <https://doi.org/10.1016/j.applthermaleng.2019.02.087>
5. C. K. Ho, J. M. Christian, A. C. Moya, J. Taylor, D. Ray, J. Kelton, "Experimental and numerical studies of air curtains for falling particle receivers" Proceedings of ESFuel-Cell2014, 2014, <https://doi.org/10.1115/ES2014-6632>
6. R. Flesch, J. Grobbel, H. Stadler, R. Uhlig, B. Hoffschmidt, "Reducing the convective losses of cavity receivers" AIP Conference Proceedings, vol. 1734, p. 030014, 2016, <https://doi.org/10.1063/1.4949066>
7. E. Alipourtarzanagh, A. Chinnici, G. J. Nathan, B. B. Dally, "Experimental investigation on the influence of an air curtain on the convective heat losses from solar cavity receivers under windy condition" AIP Conference Proceedings, vol. 2303, p. 080001, 2020, <https://doi.org/10.1063/5.0028630>
8. J. S. Kraabel, "An experimental investigation of the natural convection from a side-facing cubical cavity" ASME JSME Thermal Engineering Joint Conference. Honolulu, Hawaii, March 20-24, 1983